

Toward Wearable Energy Storage Devices: Paper-Based Biofuel Cells based on a Screen-Printing Array Structure

Isao Shitanda,^{*,[a, b]} Misaki Momiyama,^[a] Naoto Watanabe,^[a] Tomohiro Tanaka,^[a]
Seiya Tsujimura,^{*,[b, c]} Yoshinao Hoshi,^[a, b] and Masayuki Itagaki^[a, b]

A novel paper-based biofuel cell with a series/parallel array structure has been fabricated, in which the cell voltage and output power can easily be adjusted as required by printing. The output of the fabricated 4-series/4-parallel biofuel cell reached 0.97 ± 0.02 mW at 1.4 V, which is the highest output power reported to date for a paper-based biofuel cell. This work contributes to the development of flexible, wearable energy storage device.

Paper-based biofuel cells (PBFCs) are attracting increasing attention as new energy harvesting systems for self-powered biosensors, sensor tags, wearable biomedical devices, and small electrical devices.^[1–19] Cellulose paper has been used as the substrate for these electrodes, which serves as a structural and mechanical support. The PBFC is light and thin, and has several advantages such as safety during use, disposability, and cost of product.

Array-type PBFCs have great potential for improved output power.^[5,20,21] For example, an array-type PBFC has been reported in which the PBFC was constructed by stacking a paper substrate with a carbon paper-based biocathode and bioanode connected in a 3-series fashion.^[5] This cell achieved a maximum output power of 0.18 mW at 1.5 V. However, in the case of previously reported array-type PBFCs,^[5] the cell components were not fully printed on the paper substrate.

Recently, we introduced a array-type origami PBFC, which was constructed as a printable array electrode of two individual cells on one sheet of paper by screen-printing.^[21] The origami PBFC, which modulated output voltage by paper folding, exhibited almost 1 V of open-circuit voltage and 48 μ W of maximum output power.

Although great progress has been made in the research field of array-type PBFCs, several challenges still need to be addressed before practical applications can be provided. The output power and voltage of the PBFCs still need to be improved in order to directly power small medical or portable wireless transmission devices that demand higher than sub-mW sources.

However, the output power and current of a PBFC is not simply improved by the straightforward scale-up of single PBFCs. For example, the current distribution due to the influence of the internal resistance of the electrodes, solution resistance, and mass transfer of the fuel cannot be ignored as the electrode area expands (see SI). In addition, uniform immobilization of enzymes over the entire electrode becomes difficult as area is increased.

In addition, the previously reported array-type paper-based PBFCs need to be stacked or folded with other components prior to use; consequently a PBFC that does not require this complicated operational procedure before use is highly desired. The rational design of array-type PBFCs is clearly a highly important topic for realizing PBFCs as user-friendly energy harvesting devices.

To solve this problem, we introduce a novel design principle for printing high-power multi-series/parallel array PBFC structures of which the cell voltage and output power can easily be adjusted as required. By adopting a parallel structure for the array-type PBFC, the output power dramatically increases. In preliminary work, we determined the most suitable design for the series/parallel structure of a single cell of an array-type PBFC electrode using the finite element method (FEM, Figure S1, Table S1).

To the best of our knowledge, this communication is the first report that demonstrates a multi-array-type PBFC on one sheet of paper. The present PBFC, which is based on a 4-series/4-parallel printable array structure, exhibited an output power of about 1 mW, and an open circuit voltage of about 2.5 V. This conceptual model is highly applicable to the development of new low-cost and flexible energy harvesting devices.

We note that a water-repellent-treated paper substrate having good oxygen permeability is the key to successfully achieving a series/parallel PBFC structure. In the present study,

[a] Prof. I. Shitanda, M. Momiyama, N. Watanabe, T. Tanaka, Prof. Y. Hoshi, Prof. M. Itagaki
Department of Pure and Applied Chemistry
Faculty of Science and Technology
Tokyo University of Science
2641, Yamazaki, Noda, Chiba 278-8510 (Japan)
E-mail: shitanda@rs.noda.tus.ac.jp

[b] Prof. I. Shitanda, Prof. S. Tsujimura, Prof. Y. Hoshi, Prof. M. Itagaki
Research Institute for Science and Technology
Tokyo University of Science
2641 Yamazaki, Noda, Chiba 278-8510 (Japan)

[c] Prof. S. Tsujimura
Division of Material Science
Faculty of Pure and Applied Science
University of Tsukuba
1-1-1, Tennodai, Tsukuba, Ibaraki 305-8573 (Japan)
E-mail: seiya@ims.tsukuba.ac.jp

Supporting information for this article is available on the WWW under <https://doi.org/10.1002/celec.201700561>

© 2017 The Authors. Published by Wiley-VCH Verlag GmbH & Co. KGaA. This is an open access article under the terms of the Creative Commons Attribution Non-Commercial NoDerivs License, which permits use and distribution in any medium, provided the original work is properly cited, the use is non-commercial and no modifications or adaptations are made.

we found a water-repellent-treated Japanese paper to be a suitable printable substrate. This paper has a printable smooth surface^[1] and good oxygen permeability. One side of the paper was coated with a water repellent, the principal component of which consisted of silicon nanoparticles. The water-repellent-treated paper retained good oxygen permeability.

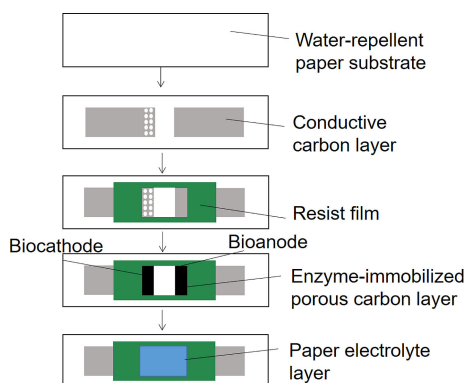


Figure 1. Fabrication process of a single cell, paper-based, biofuel cell (PBFC).

Figure 1 shows a schematic illustration of the fabrication process for the single cell; further details can be found in the Supporting Information.

The characteristics of the bioanode and biocathode were investigated independently using the three-electrode method. The bioanode or biocathode was connected to a three-electrode potentiostat (AIS/CH Instruments, Model 802B). An Ag|AgCl reference electrode and a Pt wire counter electrode were placed in the electrolyte solution. For the electrochemical measurements of the bioanode, the bioanode was soaked in the electrolyte solution, while the biocathode was floated on the electrolyte solution, to allow the supply of oxygen throughout the paper during the measurements (Figure S2). Figure 2(a) shows cyclic voltammograms (CVs) for the bioanode, in the presence and absence of 0.1 M glucose, in 1 M phosphate buffer (pH 7.0), at room temperature. Glucose is oxidized to gluconic acid in the presence of glucose oxidase (GOx), while GOx is converted to its reduced form. The reduced GOx reacts with the mediator, TTF⁺, which is reduced to tetrathiafulvalene (TTF), then diffuses and is oxidized at the carbon-electrode surface. As a result, the current increases when glucose is present in solution.^[7] Although a clear redox wave for TTF was not observed on the bioanode in the absence of glucose, a clear catalytic wave for glucose oxidation was observed in the solution containing 0.1 mol dm⁻³ glucose. The oxidation current started to flow and dramatically increased at potentials higher than 0.03 V vs. sat. KCl|Ag|AgCl during the anodic scan. The current for GO_x catalysis is clearly mediated by TTF, as evidenced from the onset potential of the catalytic current.^[17] The maximum catalytic current density at 0.23 V was 4.83 mA cm⁻².

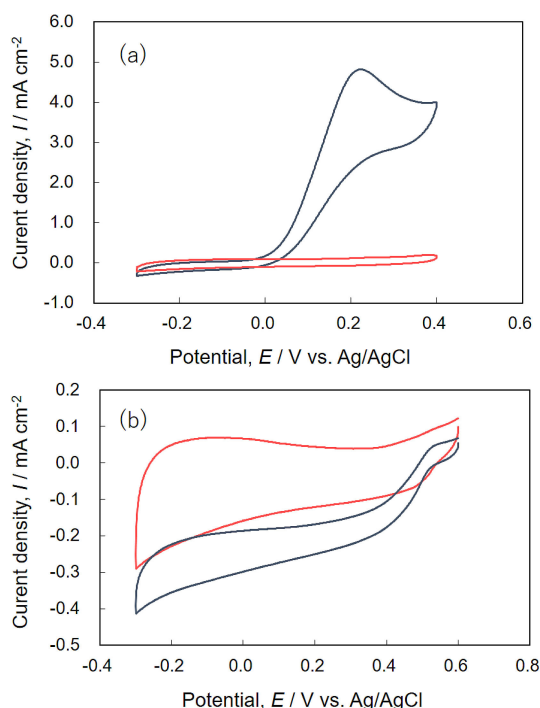


Figure 2. Cyclic voltammograms of a) GOx and TTF-immobilized porous carbon electrode (bioanode), using 1 M phosphate buffer (pH 7.0) in the presence (blue line) and absence (red line) of 100 mM glucose at room temperature. b) BOD-immobilized porous carbon electrode fabricated on the paper substrate (blue line) and on a polyimide substrate (red line) using 1 M phosphate buffer (pH 7.0) at room temperature. The scan rate was 10 mV s⁻¹. The edge of the paper was soaked in the electrolyte solution at room temperature during the measurements.

Figure 2(b) shows cyclic voltammograms for the cathode. The black line in Figure 2(b) is the CV of the present paper-based biocathode, in which the water-repellent-treated Japanese paper was used as the substrate. On the other hand, the red line is the CV of a biocathode in which a polyimide film was used as the substrate. It should be noted that the oxygen permeability of the polyimide film is quite low in comparison with that of our treated paper. Bilirubin oxidase (BOD) is known to catalyze the reduction of oxygen by a direct transfer reaction.^[7] As shown in Figure 2(b), compared to that of the polyimide-based cathode, the catalytic oxygen reduction current is dramatically increased at potentials lower than 0.54 V in the cathodic scan when the paper-based biocathode is used, since aerobic oxygen is able to penetrate into the paper and be supplied to the porous carbon layer. The maximum catalytic current density at 0.30 V was -0.41 mA cm^{-2} . On the other hand, oxygen is unable to penetrate through the polyimide surface. Consequently, the cathodic current is limited by the oxygen dissolved in the electrolyte solution.

We next fabricated single PBFCs, and arranged them into series configurations containing two and three PBFCs, as shown in Figure S3, followed by performance evaluation. In the case of the single PBFC, paper was placed between the anode and cathode surfaces (Figure S3(a)). A 1 M phosphate buffer (pH 7.0) containing 100 mM glucose was then cast onto the paper layer (Figure 1). Due to its water absorbency, the paper layer also

acts as an electrolyte container, as well as an ion exchange membrane. The output powers of the 2-series and 3-series cells were also estimated using the same procedure. The power-potential curves of these PBFCs are shown in Figure S4(a). It should be noted that all power-potential curves were measured three times for each cell and the standard deviations were calculated. To calculate the standard deviation, we made a fresh device for each measurement. The open circuit voltage (OCV) of the single cell was 0.61 V and is attributed to the difference between the onset potentials of the bioanode and biocathode. The maximum power density of the fabricated single PBFC was $76 \pm 21 \mu\text{W cm}^{-2}$. The maximum powers of the 2- and 3-series cells were 176 ± 29 and $255 \pm 54 \mu\text{W cm}^{-2}$, respectively. In addition, the OCVs of the 2- and 3-series cells were 1.2 and 1.8 V, respectively, which are about 2- and 3-times higher than that of the single cell, respectively. Figure S4(b) shows the relationship between the number of cells in the series and the maximum output power of the whole cell, and indicates that the maximum output power increases in proportion to the number of cells. From these results, we conclude that the cell voltage and output power of the cell can easily be adjusted as required using the present procedure.

Finally, we designed a new PBFC that was composed of 4-series and 4-parallel cells (16 single-cell modules) as shown in Figure 3. Details of the dimensions of this PBFC are provided in

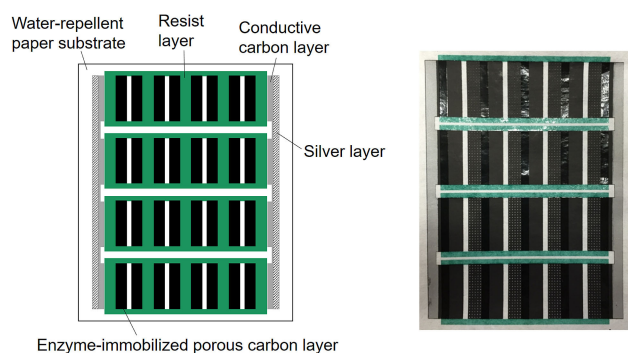


Figure 3. a) Schematic illustration and b) photograph of the 4-series/4-parallel PBFC.

Figure S5. To attain a power output in the mW region, the areas of the anode and cathode of each single cell were altered to 1 cm^2 . The FEM-simulated cell design determined that the length-to-width ratio of these electrodes should be 4; hence, each electrode was $0.5 \times 2 \text{ cm}$ in size.

In order to reduce the inner resistance of the conducting carbon layer, we used a silver connecting layer at each end of the sets of 4-series cells. The BOD of 10 U and GO_x of 200 U were immobilized onto the cathode and anode surfaces on each single cell, respectively.

The current-potential and power-potential curves of the PBFC are shown in Figure 4. The red line depicts the results from the 4-series/4-parallel cell, while the blue line shows those from the 4-series/1-parallel cell. The OCVs of both cells were 2.3 V. The maximum current and power of the 4-series/4-parallel

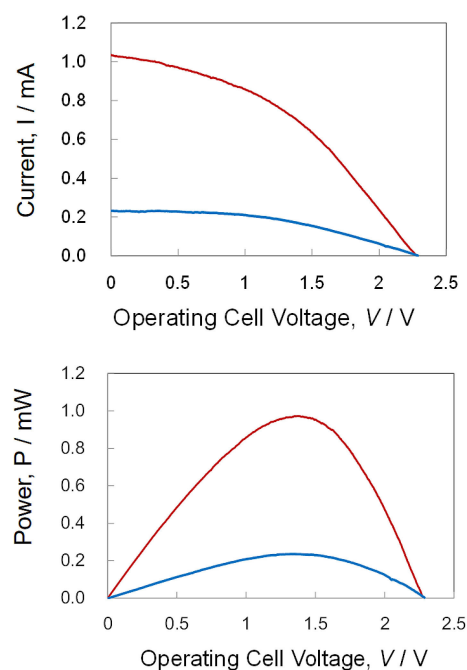


Figure 4. a) The current-potential and b) power-potential curves of the PBFCs. The red line depicts the results of the 4-series/4-parallel cell, whereas the blue line shows those of the 4-series/1-parallel cell. Experiments were conducted in pH 7.0 phosphate buffer containing 100 mM glucose at room temperature.

cell was determined to be 1.04 mA and $0.97 \pm 0.02 \text{ mW}$ at 1.4 V, respectively, four times higher than that of the 4-series/1-parallel cell (0.23 mA, $0.24 \pm 0.21 \text{ mW}$). The maximum power density of the fabricated PBFC was $60 \mu\text{W cm}^{-2}$. The maximum power and current from this cell are, to the best of our knowledge, the highest reported to date for a PBFC (Table S2).^[10–19] The output power density of the 4-series/4-parallel cell is lower than that of our previous work^[7,21] because the structure of the PBFCs are completely different. The output power and current of our PBFCs depend on the performance of the biocathode. In the case of our previous PBFCs, oxygen is directly supplied to the biocathode from the air, while in the case of our present PBFC, oxygen passes through the water-repellent paper to react at the biocathode surface. Despite this, the maximum power density was 1.7 times higher than that of a printed paper-based biofuel cell fabricated on one sheet of paper.^[20] We also demonstrated that this PBFC was able to illuminate an LED without the need for a booster circuit. (Figure S6).

In summary, we have constructed a mW performing PBFC by applying suitable porous anodic/cathodic carbon inks and array structures. The fabricated PBFC exhibited a remarkable power output of close to 1 mW ($0.97 \pm 0.02 \text{ mW}$), which, to the best of our knowledge, is the highest output power reported to date for this type of cell. The maximum power density of the fabricated PBFC was 0.06 mW cm^{-2} . The flexible, paper-based, biofuel cells are highly applicable to the development of low cost, flexible, and wearable, energy devices. In the near future, we will endeavor to fabricate a fully screen-printed PBFC prepared by enzyme-containing inks.

Acknowledgements

This work was supported by JST A-STEP (AS272S004a). I.S. acknowledges financial support from the Hosokawa Powder Technology Foundation and the Iwatani Naoji Foundation.

Conflict of Interest

The authors declare no conflict of interest.

Keywords: paper-based device · biofuel cells · biofuels · ink printing · array structure

- [1] M. J. Gonzalez-Guerrero, F. J. del Campo, J. P. Esquivel, F. Giroud, S. D. Minteer, N. Sabate, *J. Power Sources* **2016**, *326*, 410–416.
- [2] S. Li, Y. Wang, S. Ge, J. Yu, M. Yan, *Biosens. Bioelectron.* **2015**, *71*, 18–24.
- [3] C. Lau, M. J. Moehlenbrock, R. L. Arechederra, A. Falase, K. Garcia, R. Rincon, S. D. Minteer, S. Banta, G. Gupta, S. Babanova, P. Atanassov, *Int. J. Hydrogen Energy* **2015**, *40*, 14661–14666.
- [4] T. H. Nguyen, A. Fraiwan, S. Choi, *Biosens. Bioelectron.* **2014**, *54*, 640–649.
- [5] C. W. Narváez Villarrubia, C. Lau, G. P. M. K. Ciniciato, S. O. Garcia, S. S. Sibbett, D. N. Petsev, S. Babanova, G. Gupta, P. Atanassov, *Electrochim. Commun.* **2014**, *45*, 44–47.
- [6] G. Strack, S. Babanova, K. E. Farrington, H. R. Luckarift, P. Atanassov, G. R. Johnson, *J. Electrochem. Soc.* **2013**, *160*, G3178–G3182.
- [7] Shitanda, S. Kato, Y. Hoshi, M. Itagaki, S. Tsujimura, *Chem. Commun.* **2013**, *49*, 11110–11112.
- [8] Fraiwan, S. Mukherjee, S. Sundermier, H. S. Lee, S. Choi, *Biosens. Bioelectron.* **2013**, *49*, 410–414.
- [9] L. Zhang, M. Zhou, D. Wen, L. Bai, B. Lou, S. Dong, *Biosens. Bioelectron.* **2012**, *35*, 155–159.
- [10] G. P. M. K. Ciniciato, C. Lau, A. Cochrane, S. S. Sibbett, E. R. Gonzalez, P. Atanassov, *Electrochim. Acta* **2012**, *82*, 208–213.
- [11] K. Sode, T. Yamazaki, I. Lee, T. Hanashi, W. Tsugawa, *Biosens. Bioelectron.* **2016**, *76*, 20–28.
- [12] D. Pankratov, E. Gonzalez-Arribas, Z. Blumm, S. Shleev, *Electroanal.* **2016**, *28*, 1250–1266.
- [13] S. O. Garcia, Y. V. Ulyanova, R. Figueroa-Teran, K. H. Bhatt, S. Singhal, P. Atanassov, *ECS J. Solid State Sci. Technol.* **2016**, *5*, M3075–M3081.
- [14] S. Cosnier, A. J. Gross, A. Le Goff, M. Holzinger, *J. Power Sources* **2016**, *325*, 252–263.
- [15] J. Bandodkar, J. Wang, *Electroanal.* **2016**, *28*, 1188–1200.
- [16] M. Zhou, *Electroanal.* **2015**, *27*, 1786–1810.
- [17] R. C. Reid, S. D. Minteer, B. K. Gale, *Biosens. Bioelectron.* **2015**, *68*, 142–148.
- [18] D. P. Hickey, R. C. Reid, R. D. Milton, S. D. Minteer, *Biosens. Bioelectron.* **2015**, *77*, 26–31.
- [19] J. Bandodkar, W. Jia, J. Wang, *Electroanal.* **2015**, *27*, 562–572.
- [20] X. E. Wu, Y. Z. Guo, M. Y. Chen, X. D. Chen, *Electrochim. Acta* **2013**, *98*, 20–24.
- [21] Shitanda, S. Kato, S. Tsujimura, Y. Hoshi, M. Itagaki, *Chem. Lett.* **2017**, *46*, 726–728

Manuscript received: June 6, 2017

Accepted Article published: June 15, 2017

Version of record online: June 26, 2017